DOI: 10.61782/fa.2023.0773

forum acusticum 2023

A THREE-DIMENSIONAL MULTI-GRID STAGGERED FINITE-DIFFERENCE TIME-DOMAIN METHOD FOR UNDERWATER TARGET ACOUSTIC SCATTERING

Roberto Sabatini[1] **Yan Pailhas**[2*] **Alessandro Monti**[2]
Angeliki Xenaki[2] **Paul Cristini**[3]
[1] Embry-Riddle Aeronautical University, Daytona Beach, Florida, USA
[2] Centre for Maritime Research and Experimentation, La Spezia, Italy
[3] Aix-Marseille University, CNRS, Centrale Marseille, LMA, Marseille, France

ABSTRACT

Staggered second-order finite-difference time-domain (FDTD) schemes are commonly used to solve the linearized equations of continuum mechanics for the acoustic scattering of objects. They are simple to implement and parallelize, a key feature in the era of exascale computing. However, their low resolution due to their formal low order and stair-step representation of media interfaces is a major drawback. This requires a fine grid resolution to reduce numerical dissipation and dispersion, leading to high computational costs in three-dimensional configurations. To counteract this issue, we propose a multi-grid FDTD method. Here, the mesh is refined locally in a region of interest, while a coarser grid is employed in the remaining domain. In the fine grids, the staggered FDTD is used, and in the coarse grid, higher-order staggered schemes are included to account for the decreased resolution due to the larger spacing. High-order interpolation is used to match the solutions at the grid interfaces. The effectiveness of the technique will be tested on well-known benchmark test.

Keywords: *Multi-grid, staggered FDTD, iso-resolution.*

**Corresponding author*: *yan.pailhas@cmre.nato.int.*

1. INTRODUCTION

The acoustic scattering by objects embedded in a single or multi-media domain is a challenging problem that requires the use of numerical methods. The most common approaches are the semi-analytical techniques, such as the elastodynamic geometric theory of diffraction [1] and the boundary element method [2], and the purely numerical techniques, such as the finite-element methods [3, 4] and finite-difference time-domain (FDTD) methods [5–7]. The purely numerical techniques are more flexible when dealing with the scattering from complex objects and interfaces, since the surfaces can be tackled directly without the need for complicated analytical treatments, if they exist. In particular, the FDTD methods have an advantage over some of the techniques mentioned in assigning the distribution of the material properties and in defining the geometries and the interfaces of the objects. In fact, these methods combine simplicity and ease of implementation and parallelization that, in the era of exascale computing, is certainly one of the most important features to consider. Among the FDTD methods, the staggered second-order FDTD scheme (equivalent to the elastodynamic finite integration technique, EFIT [6, 8]) is one of the most adopted and successful techniques to tackle the linearized equations of continuum mechanics for the acoustic scattering of objects. The advantage of the grid staggering is that it implicitly guarantees the direct enforcement of the boundary conditions. However, as any other finite-difference scheme, the staggered second-order FDTD scheme suffers of an inherent low resolution, due to their formal low-order of accuracy, and poorly describes the interfaces between media (e.g.

object/water) with a stair-step representation. Thereby, a staggered second-order FDTD scheme requires high-resolution grids to capture the small-scale features of the scattering by the objects (considering the vast range of scales involved) and to reduce the numerical dissipation and dispersion. These high-resolution grids lead to enormous computational costs in three-dimensional configurations. To avoid this problem, we propose a staggered FDTD multi-grid method where high-resolution grids are embedded in the coarse mesh to target the presence of objects and interfaces. The finer grids are coupled to the coarser grid by exchanging boundary conditions at the interface between them. Interpolation is needed since the high-resolution grids refine the mesh locally in a discontinuous manner. The embedding procedure allows for accurate and efficient simulations of complex phenomena with a wide range of scales [9–11].All the methods introduced so far in the acoustic analysis present a discontinuity of resolution between the coarse and the fine grid, since no numerical trick is introduced to increase the resolution in the coarse lattice and the order of the numerical schemes is maintained identical across them. This affects the quality of the solution on the coarser grid due to the intrinsic lower-resolution spacing. To overcome this problem, we propose an iso-resolution method, where two different schemes are adopted between the two different regions. This allows having a uniform resolution on the whole domain. Specifically, in the fine grids, the aforementioned second-order staggered FDTD is employed whereas in the coarse grid higher-order staggered schemes are used to compensate the decrease in resolution due to the larger spacing. To complete the treatment, a high-order interpolation at the grid interfaces is employed to match the solutions on the two grids, thus reducing the artificial dispersion introduced by the lattice discontinuity.

2. METHODOLOGY

We consider the three-dimensional acoustic and elastic linearized wave equations

$$\begin{aligned} \frac{\partial v_i'}{\partial t} &= \frac{1}{\overline{\rho}} \frac{\partial \sigma_{ij}'}{\partial x_j} + f_i, \\ \frac{\partial \sigma_{ij}'}{\partial t} &= \overline{\lambda} \frac{\partial v_i'}{\partial x_i} \delta_{ij} + \overline{\mu} \left(\frac{\partial v_j'}{\partial x_i} + \frac{\partial v_i'}{\partial x_j} \right) + G_{ij}, \end{aligned} \tag{1}$$

where $\overline{\rho}$ is the density of the medium, $\overline{\lambda}$ and $\overline{\mu}$ are the Lamé parameters, v_i' is the perturbation of the ith component of the velocity vector, σ_{ij}' is the perturbation of the ijth component of the stress tensor, f_i and G_{ij} are source terms. The subscripts $i \in [1,2,3]$ and $j \in [1,2,3]$ indicate the Cartesian directions $x_1 = x$, $x_2 = y$ and $x_3 = z$, where the latter indicates the vertical direction, taken positively from the bottom of the domain and the former two are the horizontal directions, respectively. The set of equations (1) are numerically solved in a cubic box whose dimension depends on the physics of the problem at hand. In a simplified scenario of interest for this work, the computational box generally includes a multi-media domain, Ω_1 (a fluid at rest, e.g. water) and Ω_2 (e.g. a scattering object), and a localized acoustic source. At the interfaces between two different media, the following constraints must be verified: 1) continuity of the normal velocity; 2) continuity of the normal stress; 3) tangential stress must vanish (fluid-solid interface). The system (1) is discretized on a uniform Cartesian grid with a staggered FDTD [6]. The time discretization is uniform on the whole domain, with a second-order accuracy finite-difference scheme. The spatial order of accuracy varies with the choice of the scheme employed in the coarse and fine grids. Specifically, we adopt the standard second-order scheme in the fine grid, whereas in the coarse grid the scheme selection is affected by the ratio r between the coarse and the fine spacing. Note that in the method implemented in this work, only odd ratios can be chosen to minimize the number of interpolations needed (staggered grid). To select the appropriate scheme that guarantees an iso-resolution over the whole computational box, we introduce a criterion based on a threshold that limits the numerical dispersion introduced by the numerical schemes as a function of the maximum resolved scales. The threshold is chosen empirically, such that the numerical dispersion is lower than a small value ϵ. The choice of ϵ can influence the order of the scheme in the coarse grid. For the sake of simplicity, we introduce the mono-dimensional relation for P-waves that links the numerically solved frequency ω^* and the relative grid spacing Δ,

$$\omega^* \Delta t = 2 \arcsin \left[\mathrm{CFL} \sum_{m=1}^{M} a_m \sin \left[\frac{k\Delta}{2} (2m-1) \right] \right], \tag{2}$$

where M is the number of points of the one-sided stencil that, for even-order schemes, defines the order of the scheme itself $N = 2M$. The coefficients a_m are the stencil coefficients of the numerical scheme chosen, Δt is the time-step, k is the wavenumber and CFL is the Courant number that relates Δt and Δ with the wave velocity c, i.e. $\mathrm{CFL} = \Delta t\, c/\Delta$. The analytical frequency ω, instead,

can be written as $\omega\Delta t = \text{CFL}\, k\Delta$. The aforementioned threshold that limits the numerical dispersion can be defined as $\mathcal{T} = |\omega - \omega^*|\Delta t$, and it is set to $\mathcal{T} = 5 \times 10^{-4}$. In this way, to obtain an iso-resolution among all the computational points, an eight-order scheme in the coarse grid is employed if $r = 3$ (a twelfth-order scheme if $r = 5$). To avoid further numerical dispersion, a high-order Lagrangian interpolation (> 4) is employed at the interface between the grids to calculate boundary values for the fine grid and to reduce the numerical dispersion introduced by the mesh discontinuity. Finally, the coarse nodes shared with the fine grid are updated through the values computed on the latter. The properties of the media are evaluated on every grid cell in the same place as the normal stresses and are averaged among the neighbouring points when an intermediate value is needed (e.g., density for the velocity components integration and Lamé parameters for the shear stress components integration). The point-wise definition of the properties of the materials directly define the different objects belonging to the computational domain, with no particular treatment needed to outline the interfaces. At the boundaries of the computational box, we implement the perfectly matched layer (PML) method introduced in Calvo *et al.* [7] to avoid artificial reflections. The PML absorbs and dampens all the waves coming from inner domain in a layer of 60 points in this work. Finally, the acoustic source is a spherical source whose implementation is extensively described in our previous work [12]. Its location does not influence the design of the multi-grid method. The code is written with NVIDIA's CUDA paradigms to parallelly run on a single GPU device.

3. PRELIMINARY RESULTS

To assess the validity of the method, a three-dimensional numerical experiment is carried out. A spherical Ricker pulse with Gaussian aperture is applied to the right-hand-side of the normal stresses equations (1). The implementation of the source comes from the integral form of the Ricker pulse with Gaussian aperture described in our previous work (extended-source [12]). The pulse adopted here, with central frequency $f_c = 25000$ Hz, central time $t_c = 0.1$ ms and standard deviation of the Gaussian aperture $\alpha = 0.012$ m, is emitted from a source centred in $(x, y, z) = (0.5, 1.0, 1.0)$ m and is scattered by a solid sphere with radius $R = 0.1$ m centred in $(x, y, z) = (1.3, 1.0, 1.0)$ m. The sphere has density $\overline{\rho}_s = 2700\,\text{kg}\,\text{m}^{-3}$, speed of the P-waves $\overline{c}_p = 6420\,\text{m}\,\text{s}^{-1}$, and speed of the S-waves $\overline{c}_s = 3040\,\text{m}\,\text{s}^{-1}$, and is immersed in a fluid with density $\overline{\rho}_w = 1000\,\text{kg}\,\text{m}^{-3}$ and speed of sound $\overline{c}_w = 1500\,\text{m}\,\text{s}^{-1}$. The simulation is carried out on computational box with size $L_x \times L_y \times L_z = 1.9$ m$\times 1.9$ m$\times 1.9$ m. The coarse grid uniformly discretizes the domain with a Cartesian lattice having $N_x \times N_y \times N_z = 640 \times 640 \times 640$ points, yielding to a resolution $\Delta = 2.97 \times 10^{-3}$ m. The finer grid, instead, is built around the sphere to have a better description of the interfaces and it is defined by $r = \Delta_c/\Delta_f = 3$, where the subscripts c and f indicate the coarse and fine grid respectively. This brings to a resolution $\Delta_f = 1 \times 10^{-3}$ m and a number of points $M_x \times M_y \times M_z = 808 \times 808 \times 808$. The size of the box for the finer grid is chosen such that is contains indicatevely twice the typical length of the scattered object (i.e., twice the diameter of the sphere). As seen in the previous section, the choice of $r = 3$ leads to the use of the eight-order scheme in the coarse grid and, to avoid artificial reflections, an eight-order Lagrangian interpolation is employed at the interfaces between the two grids. The time-step is defined through the condition $CFL = 0.4$ tuned on Δ_f and $\overline{c}_p$, resulting in $\Delta t = 6.1750^{-5}$ ms. The results are shown in Figure 1, where two instantaneous snapshots of the stress field σ_{yy} are shown together with σ_{yy} signal recorded on a probe placed in the fluid. The signal is then Fourier transformed and the amplitude of the Fourier coefficients is compared to the analytical solution with a very good agreement in the range of frequencies of interest, i.e. $f \leq 70000$ Hz. In the figure, the location of the fine grid is highlighted with a red box. Note that without the multi-grid method, an equivalent resolution Δ_f would require $N_x \times N_y \times N_z = 1920 \times 1920 \times 1920$.

4. CONCLUSIONS

In this work, we implemented a novel multi-grid method that guarantees an iso-resolution on the whole computational domain. To obtain the iso-resolution, we increase the order of the scheme adopted for the discretization of the acoustic and elastic linearized wave equations on the coarse grid. The choice of the scheme is based on the criterion defined by the comparison between the numerical resolution and the analytical. To assess the quality of the method, we carried out a benchmark test and we show that the numerical solution agrees with the analytical one in the range of frequencies of interest.

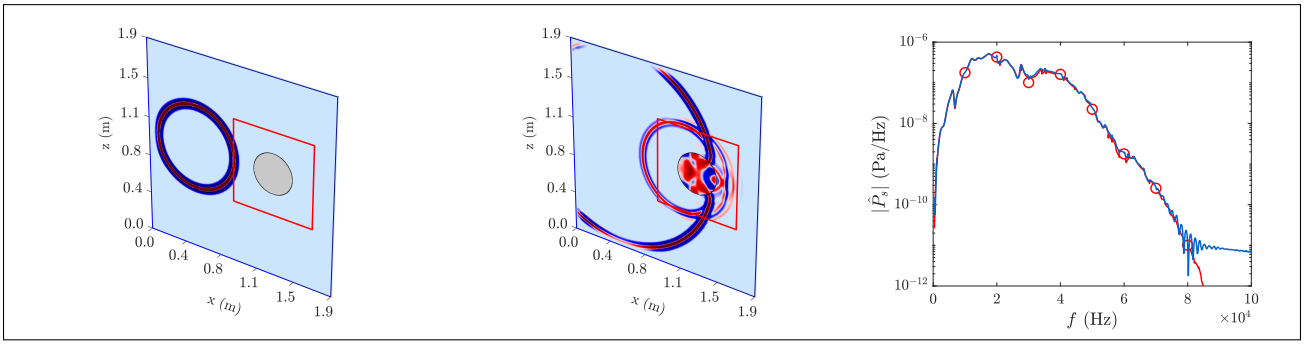

Figure 1. Left and mid panels: two-dimensional slice at $y = 1$ m of the instantaneous stress fields σ_{yy} at $t = 0.37$ ms and $t = 0.74$ ms. Right panel: amplitude of the Fourier coefficients of the σ_{yy} signal recorded at $(x, y, z) = (1.3, 1.0, 1.3)$ m (blue line) compared with the analytical solution computed at the same location (red line with markers).

5. ACKNOWLEDGMENTS

This work was performed under the Project SAC000E04-High-Resolution Low-Frequency Synthetic Aperture Sonar (HRLFSAS) of the STO-CMRE Programme of Work, funded by the NATO Allied Command Transformation.

6. REFERENCES

[1] J. D. Achenbach, A. K. Gautesen, and H. McMaken, "Ray methods for waves in elastic solids: with applications to scattering by cracks," 1982.

[2] A. Seybert and T. Wu, *Acoustic modeling: Boundary element methods*. New York: Wiley, 1998.

[3] R. Ludwig and W. Lord, "A finite-element formulation for the study of ultrasonic ndt systems," *IEEE transactions on ultrasonics, ferroelectrics, and frequency control*, vol. 35, no. 6, pp. 809–820, 1988.

[4] D. S. Burnett, *Finite element analysis: from concepts to applications*. Prentice Hall, 1987.

[5] J. Virieux, "P-SV wave propagation in heterogeneous media: Velocity-stress finite-difference method," *Geophysics*, vol. 51, no. 4, pp. 889–901, 1986.

[6] P. Fellinger, R. Marklein, K. J. Langenberg, and S. Klaholz, "Numerical modeling of elastic wave propagation and scattering with efit—elastodynamic finite integration technique," *Wave motion*, vol. 21, no. 1, pp. 47–66, 1995.

[7] D. Calvo, K. Rudd, M. Zampolli, W. Sanders, and L. Bibee, "Simulation of acoustic scattering from an aluminum cylinder near a rough interface using the elastodynamic finite integration technique," *Wave Motion*, vol. 47, no. 8, pp. 616–634, 2010.

[8] F. Schubert, A. Peiffer, B. Köhler, and T. Sanderson, "The elastodynamic finite integration technique for waves in cylindrical geometries," *The Journal of the Acoustical Society of America*, vol. 104, no. 5, pp. 2604–2614, 1998.

[9] C. Jastram and A. Behle, "Acoustic modelling on a grid of vertically varying spacing1," *Geophysical prospecting*, vol. 40, no. 2, pp. 157–169, 1992.

[10] J. Kristek, P. Moczo, K. Irikura, T. Iwata, H. Sekiguchi, K. Kudo, H. Okada, and T. Sasatani, "The 1995 Kobe mainshock simulated by the 3D finite differences," *The Effects of Surface Geology on Seismic Motion*, vol. 3, pp. 1361–1368, 1999.

[11] J. Kristek, P. Moczo, and M. Galis, "Stable discontinuous staggered grid in the finite-difference modelling of seismic motion," *Geophysical Journal International*, vol. 183, no. 3, pp. 1401–1407, 2010.

[12] R. Sabatini, Y. Pailhas, A. Xenaki, A. Monti, and P. Cristini, "Far-field analytical solutions of the non-homogeneous helmholtz and wave equations for spatially non-localized sources," *JASA Express Letters*, vol. 3, no. 2, p. 022401, 2023.